Figures and tables for "Spatiotemporally consistent global dataset of the GIMMS Leaf Area Index (GIMMS LAI4g) from 1982 to 2020"

Sen Cao[1,2,†], Muyi Li[1,†], Zaichun Zhu[1,2,*], Junjun Zha[1], Weiqing Zhao[1], Zeyu Duanmu[1], Jiana Chen[1], Yaoyao Zheng[1], Yue Chen[1]

[1]School of Urban Planning and Design, Shenzhen Graduate School, Peking University, Shenzhen 518055, China

[2]Key Laboratory of Earth Surface System and Human—Earth Relations, Ministry of Natural Resources of China, Shenzhen Graduate School, Peking University, Shenzhen 518055, China.

[†]These authors contributed equally to this work

Correspondence: Zaichun Zhu (zhu.zaichun@pku.edu.cn)

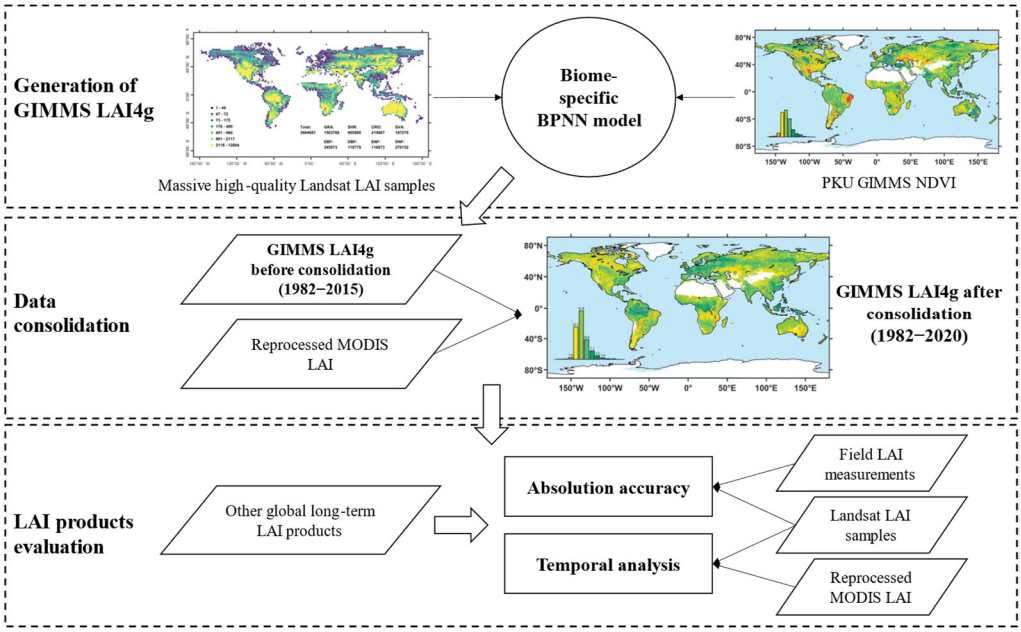

Figure 1. Schematic diagram of the generation and evaluation of the GIMMS LAI4g product.

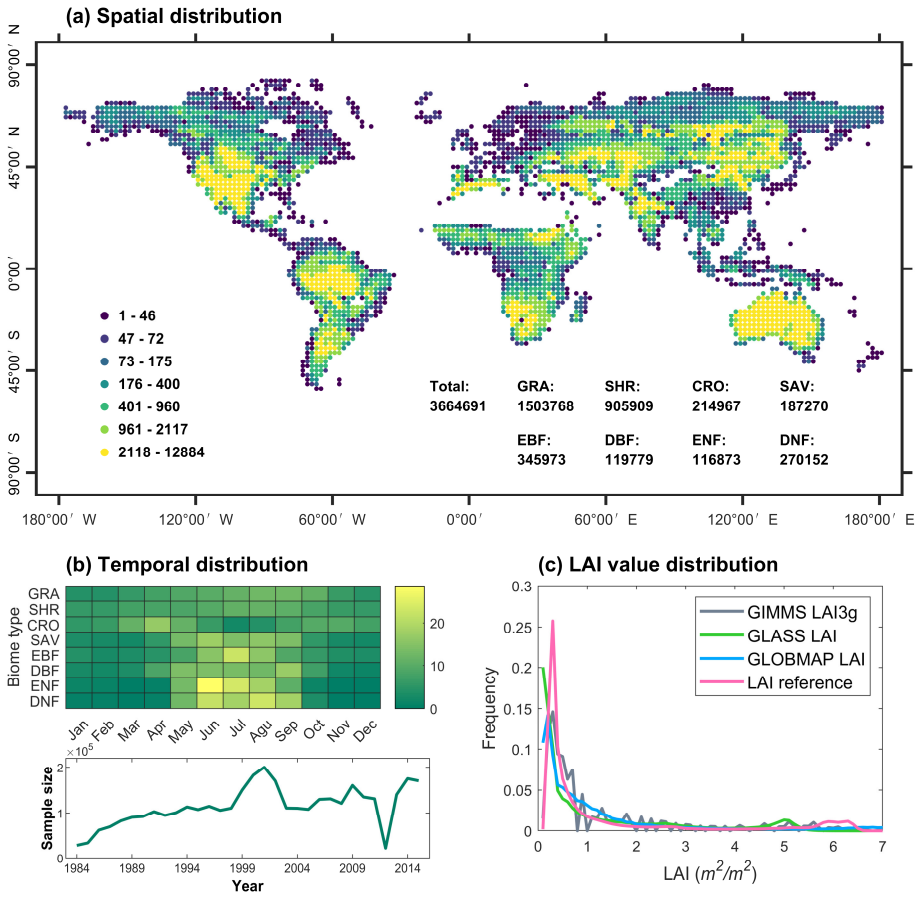

Figure 2. Spatial and temporal distribution of the LAI reference data. (a) The global distribution of LAI samples in 2° grids. The LAI sample size for each vegetation is listed. (b) The temporal distribution of LAI samples for the eight vegetation biome types and the annual variation of LAI sample size. (c) The distribution of LAI values in percentage (bin width = 0.1) for Landsat LAI samples, GIMMS LAI3g, GLASS LAI, and GLOBMAP LAI. It should be noted that 40,000 Reprocessed MODIS LAI samples were introduced at locations and months when Landsat LAI samples were scarce.

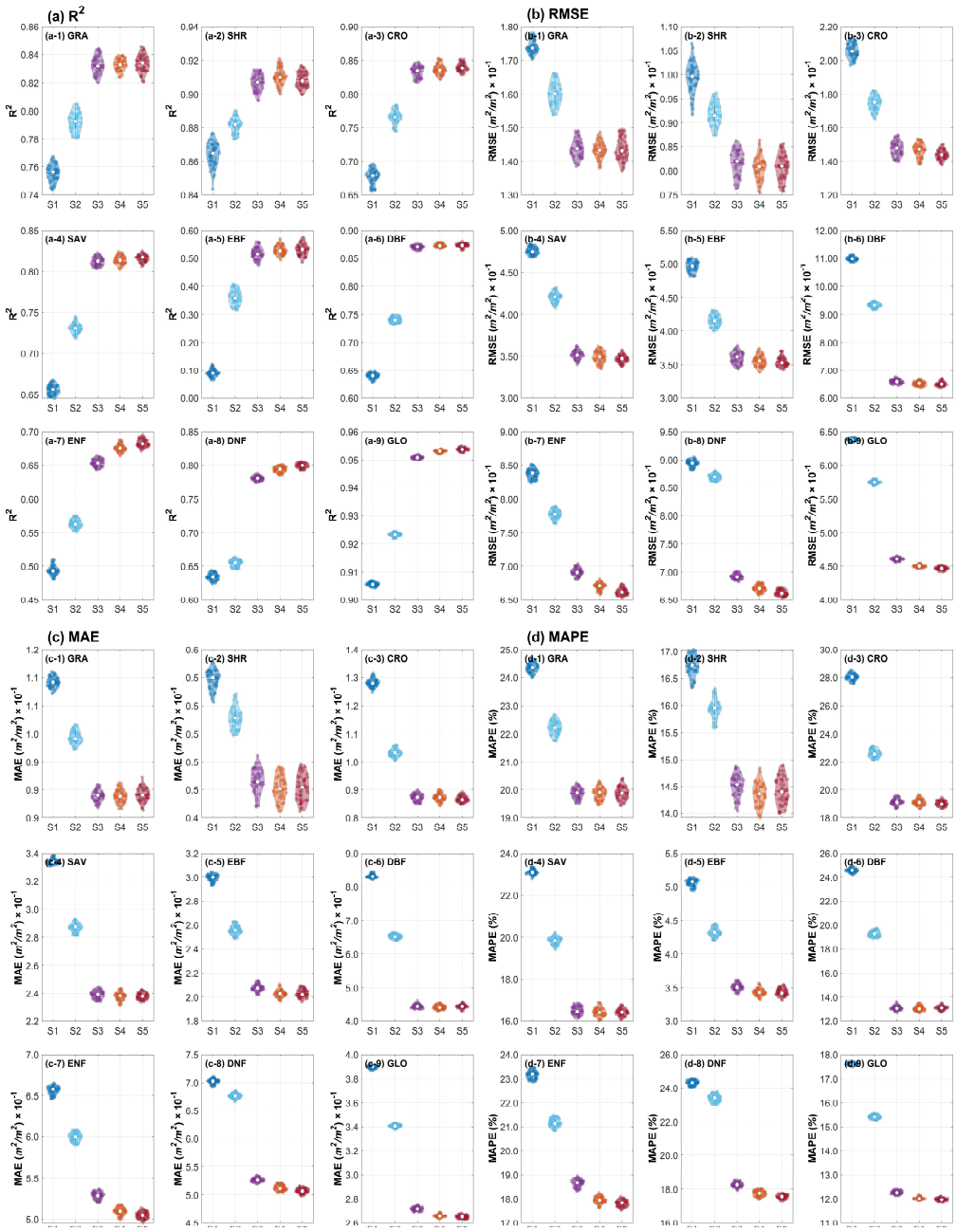

Figure 3. Performance of different combinations of explanatory variables (S1 to S5) in BPNN models for each vegetation biome. (a), (b), (c), and (d) shows the R^2, RMSE, MAE, and MAPE, respectively, calculated based on Landsat LAI samples. GLO represents the global vegetation biome. The combinations of explanatory variables are (S1) NDVI alone; (S2) NDVI and spatial information (longitude and latitude); (S3) NDVI, spatial information, and temporal information (month); (S4) NDVI, spatial information, temporal information, and NOAA satellite number; and (S5) NDVI, spatial information, temporal information, NOAA satellite number and years since its launch.

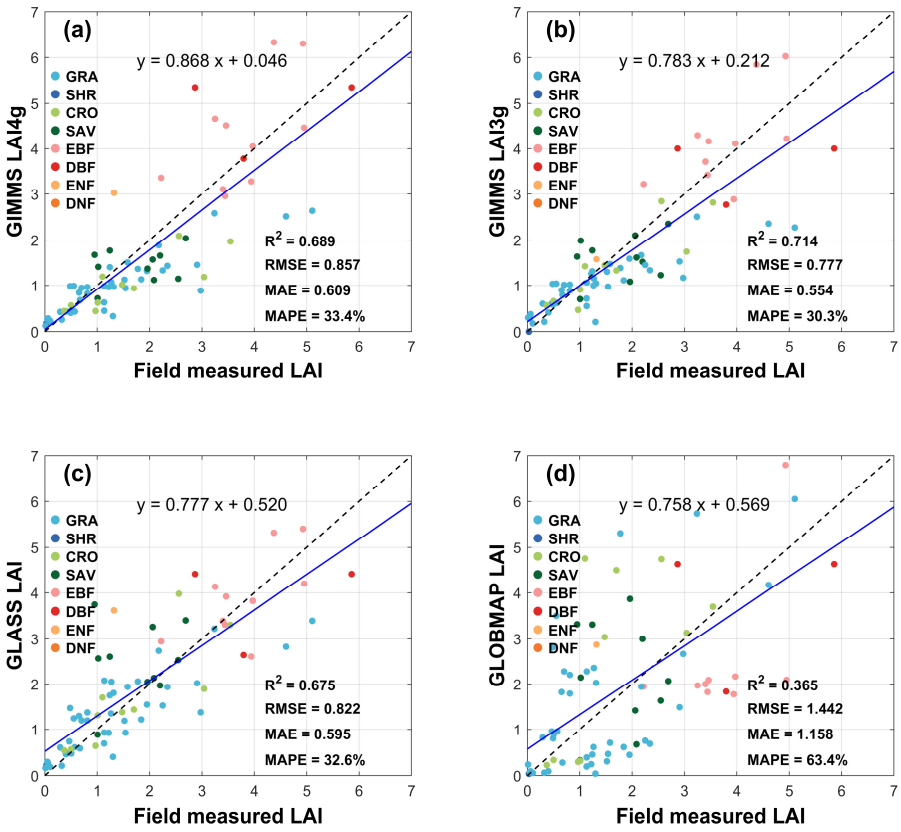

Figure 4. Validation of the (a) GIMMS LAI4g, (b) GIMMS LAI3g, (c) GLASS LAI, and (d) GLOBMAP LAI products using 113 field LAI measurements from 49 sites in the projects of BELMANIP 2.1, DIRECT 2.1, and ORNL. Sites of different vegetation biome types are marked by colors. The error metrics are R^2, RMSE, MAE, and MAPE. The blue fitting lines and dashed 1:1 lines are drawn.

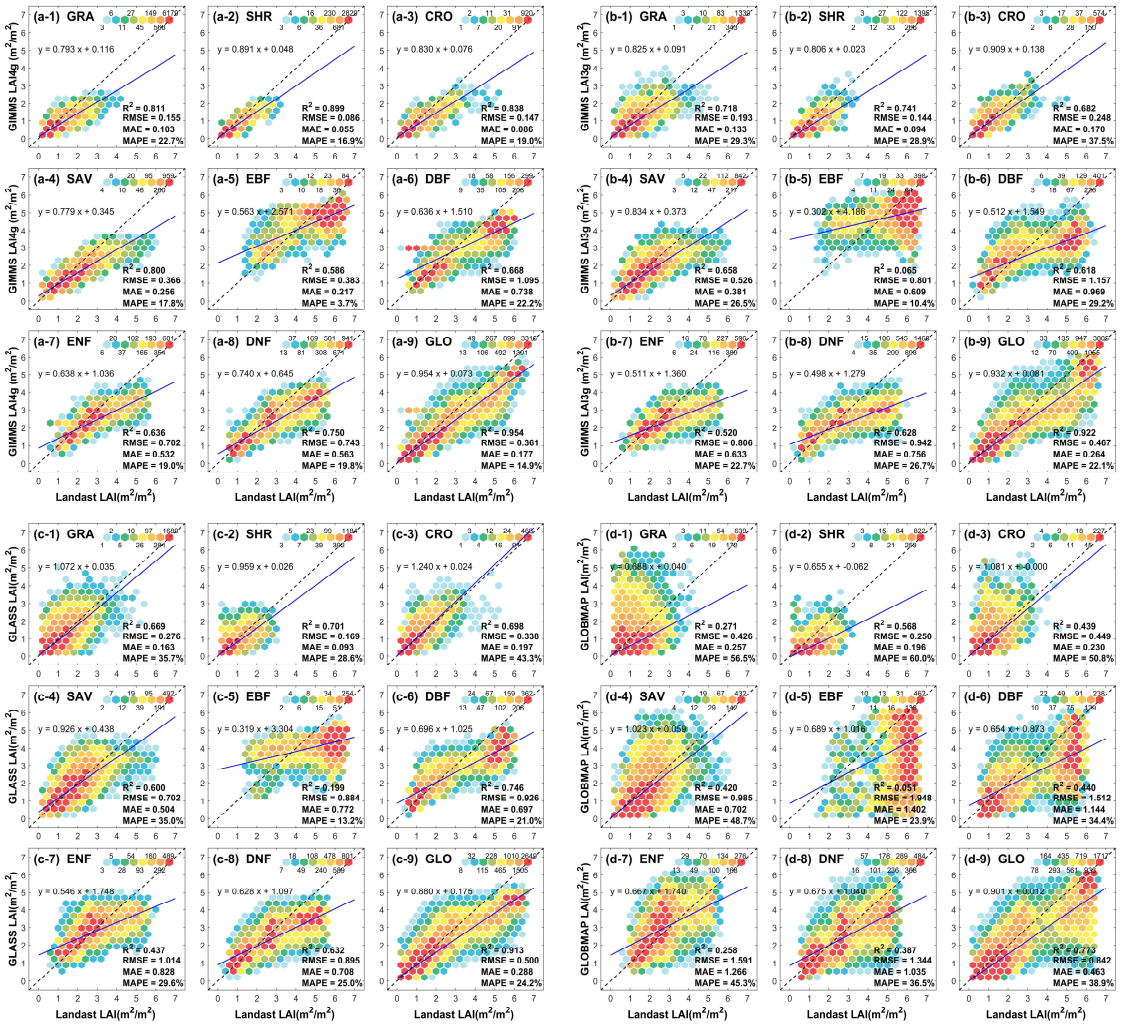

Figure 5. Validation of the (a) GIMMS LAI4g, (b) GIMMS LAI3g, (c) GLASS LAI, and (d) GLOBMAP LAI products in different vegetation biomes using Landsat LAI samples from 1984 to 2015. The error metrics are R^2, RMSE, MAE, and MAPE. GLO represents the global vegetation biome. The color of the dots represents LAI value frequencies in a 0.5 (m^2/m^2) interval.

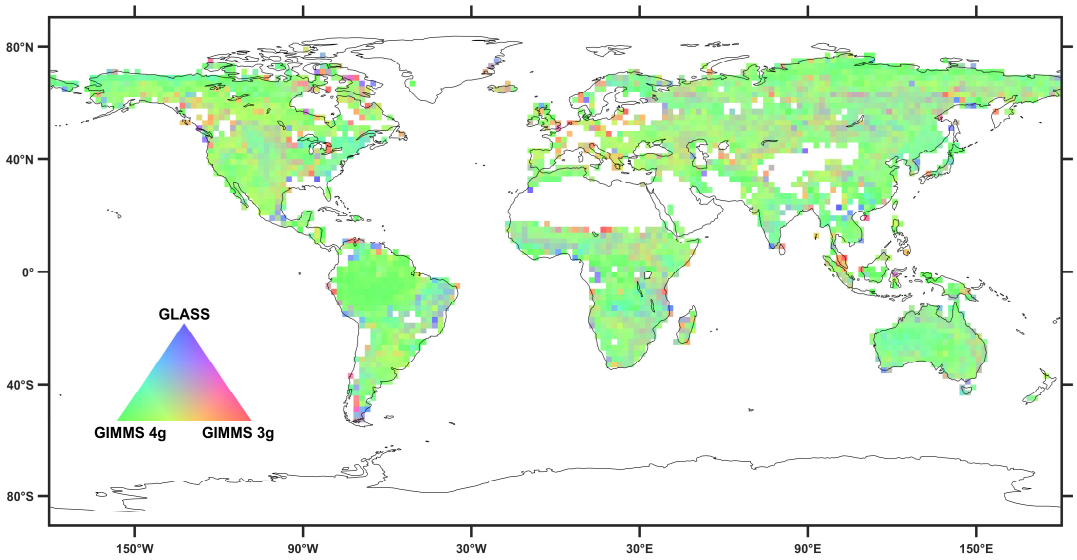

Figure 6. Dominance map of the GIMMS LAI3g, GIMMS LAI4g, and GLASS LAI based on their MAE. The map was drawn in 2° × 2° grids whose colors were composed of reciprocal averages of MAE from the GIMMS LAI4g (green), GIMMS LAI3g (red), and GLASS LAI (blue). Non-vegetated grids and grids with small Landsat LAI sample size (< 100) were filled white. A greener grid, for example, indicates that the GIMMS LAI4g has a lower MAE (or a higher absolute LAI accuracy).

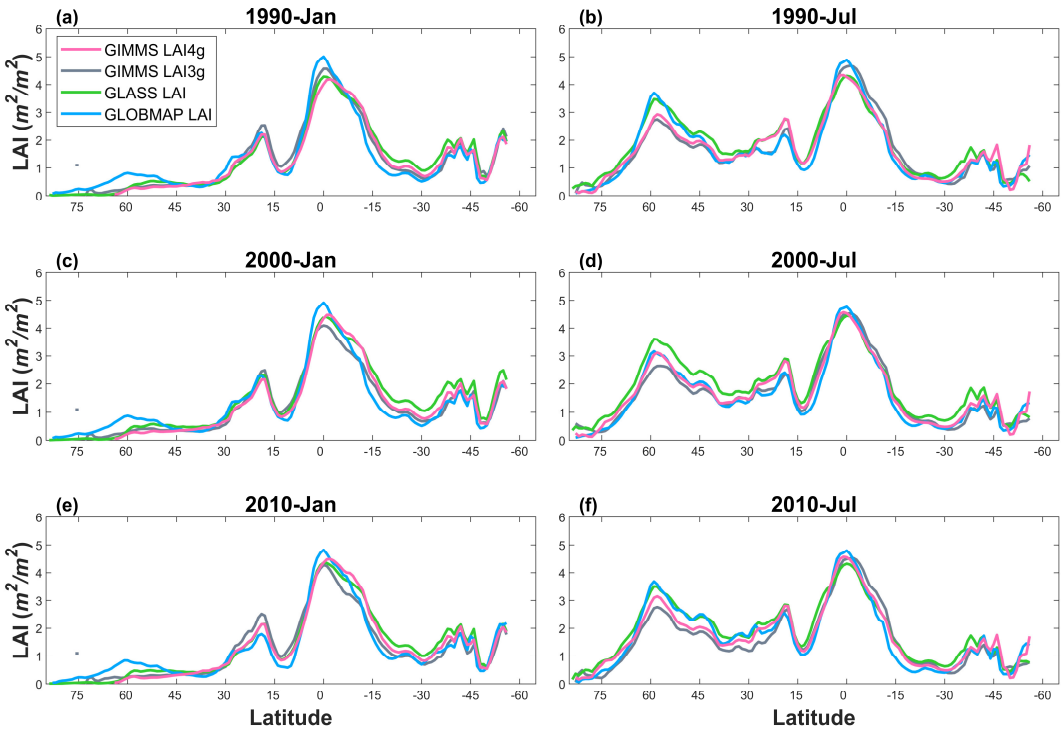

Figure 7. Inter-comparison of spatially averaged LAI along latitude between the GIMMS LAI4g, GIMMS LAI3g, GLASS LAI, and GLOBMAP LAI in January and July of the years 1990, 2000, and 2010. The spatial average was calculated at an interval of 1°.

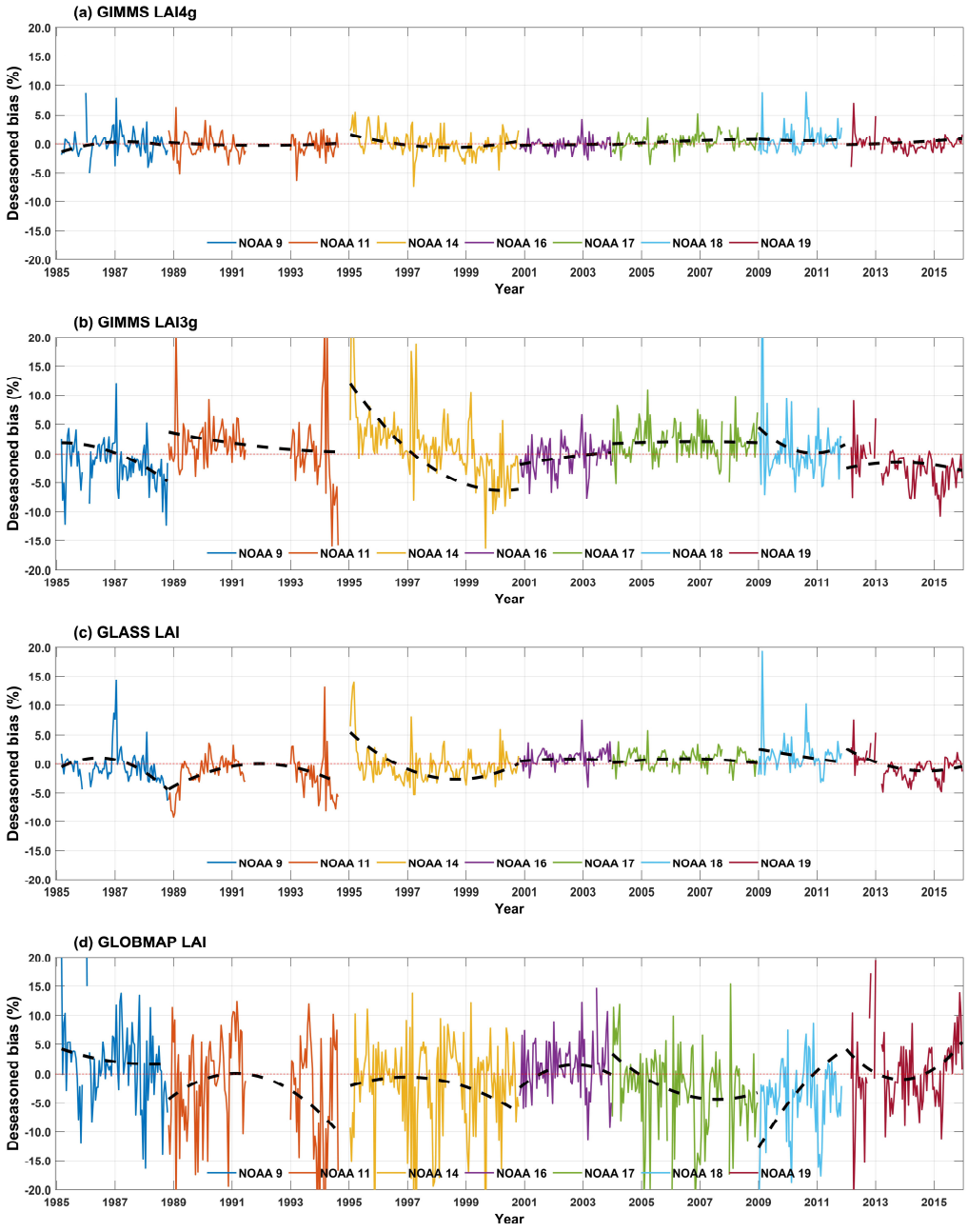

Figure 8. Temporal variations of LAI bias% in EBF for (a) the GIMMS LAI4g, (b) GIMMS LAI3g, (c) GLASS LAI, and (d) GLOBMAP LAI. The black dash line represents the interannual trend extracted by the EEMD method. Values from different NOAA satellite missions were distinguished with colors.

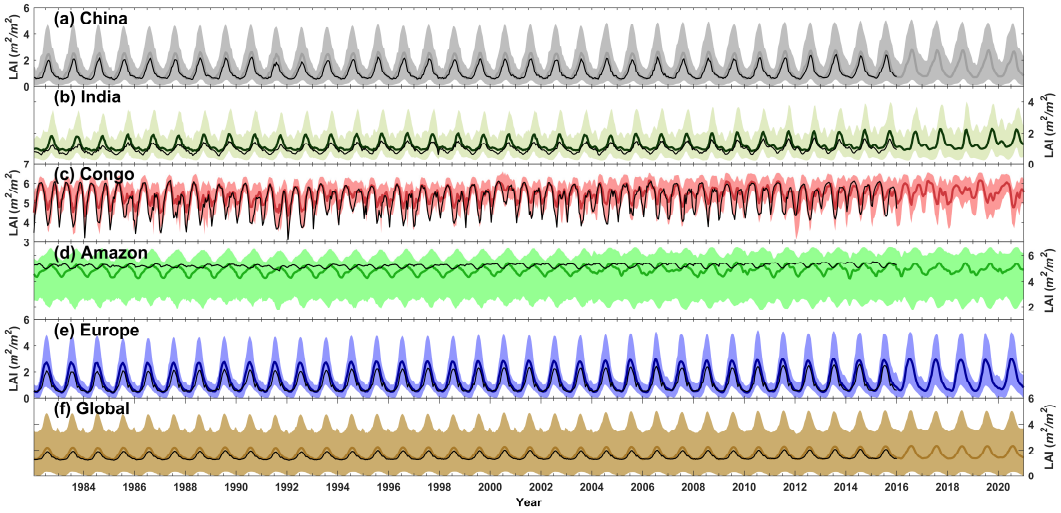

Figure 9. Temporal variations of the GIMMS LAI4g during 1982−2020 in selected hotspot regions of China (a), India (b), Congo (c), Amazon (d), and Europe (e) and at the global scale (f). GLO represents the global vegetation biome. The bold colored line represents the LAI average of GIMMSLAI4g after data consolidation, with shadow covering the value range between 10% and 90% quantiles. The thin black line represents the LAI average of GIMMSLAI4g before consolidation. It should be noted that the GIMMS LAI4g after consolidation shared the same footprint with the Reprocessed MODIS LAI after the year 2004.

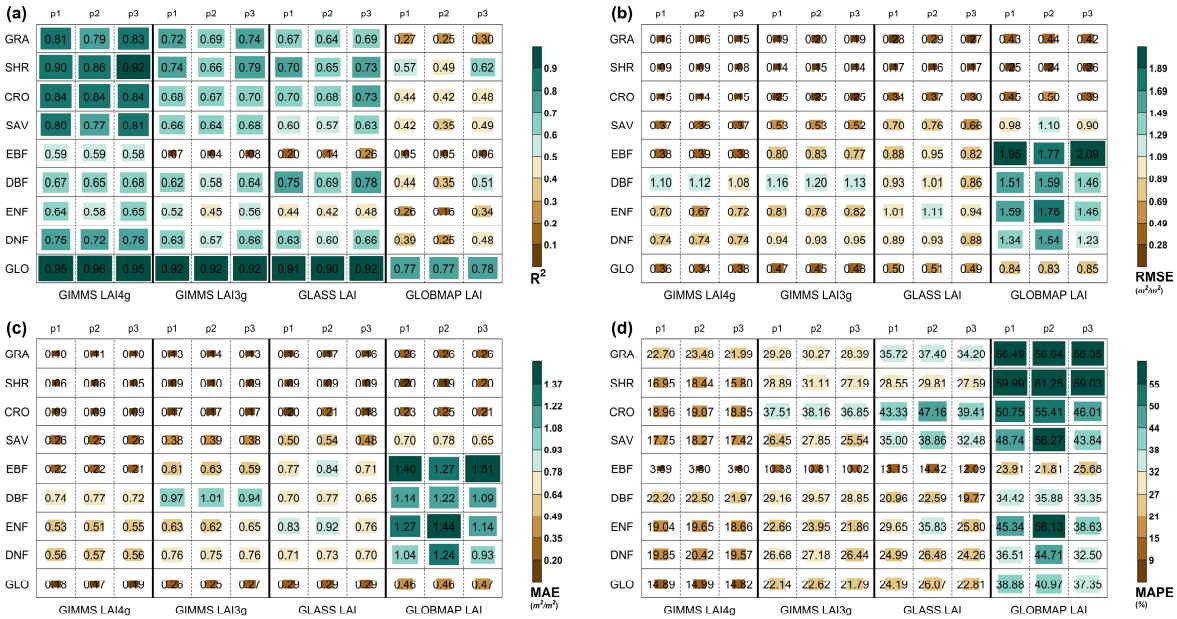

Figure 10. Temporal consistencies between different periods for the global LAI products. The global LAI products include GIMMS LAI4g, GIMMS LAI3g, GLASS LAI, and GLOBMAP LAI). The periods are 1984−2015 (p1), 1984−2000 (p2), and 2001−2015 (p3). The consistencies were evaluated at the biome level using R^2 (a), RMSE (b), MAE (c), and MAPE (d) calculated based on Landsat LAI samples. GLO represents the global vegetation biome.

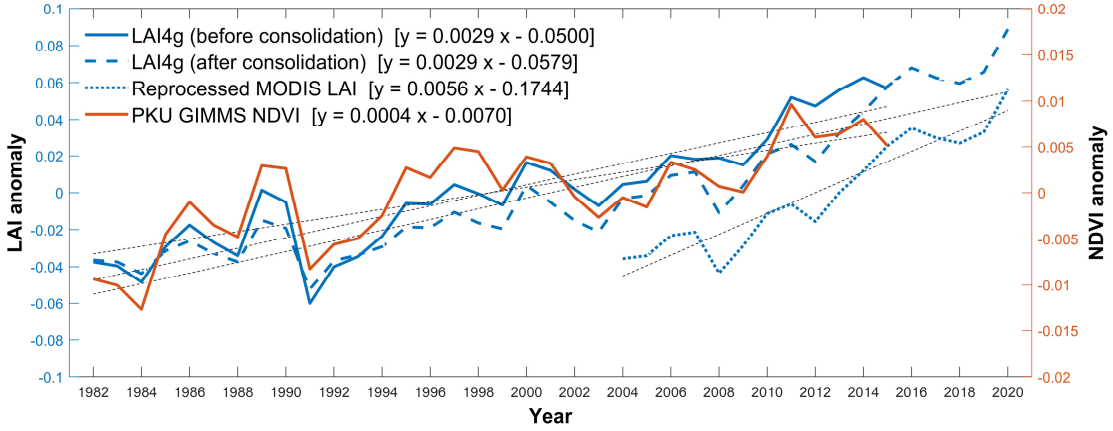

Figure 11. Annual anomalies and trends of GIMMS LAI4g before consolidation (1982−2015), GIMMS LAI4g after consolidation (1982−2020), Reprocessed MODIS LAI (2004−2020), and PKU GIMMS NDVI (1982−2015).

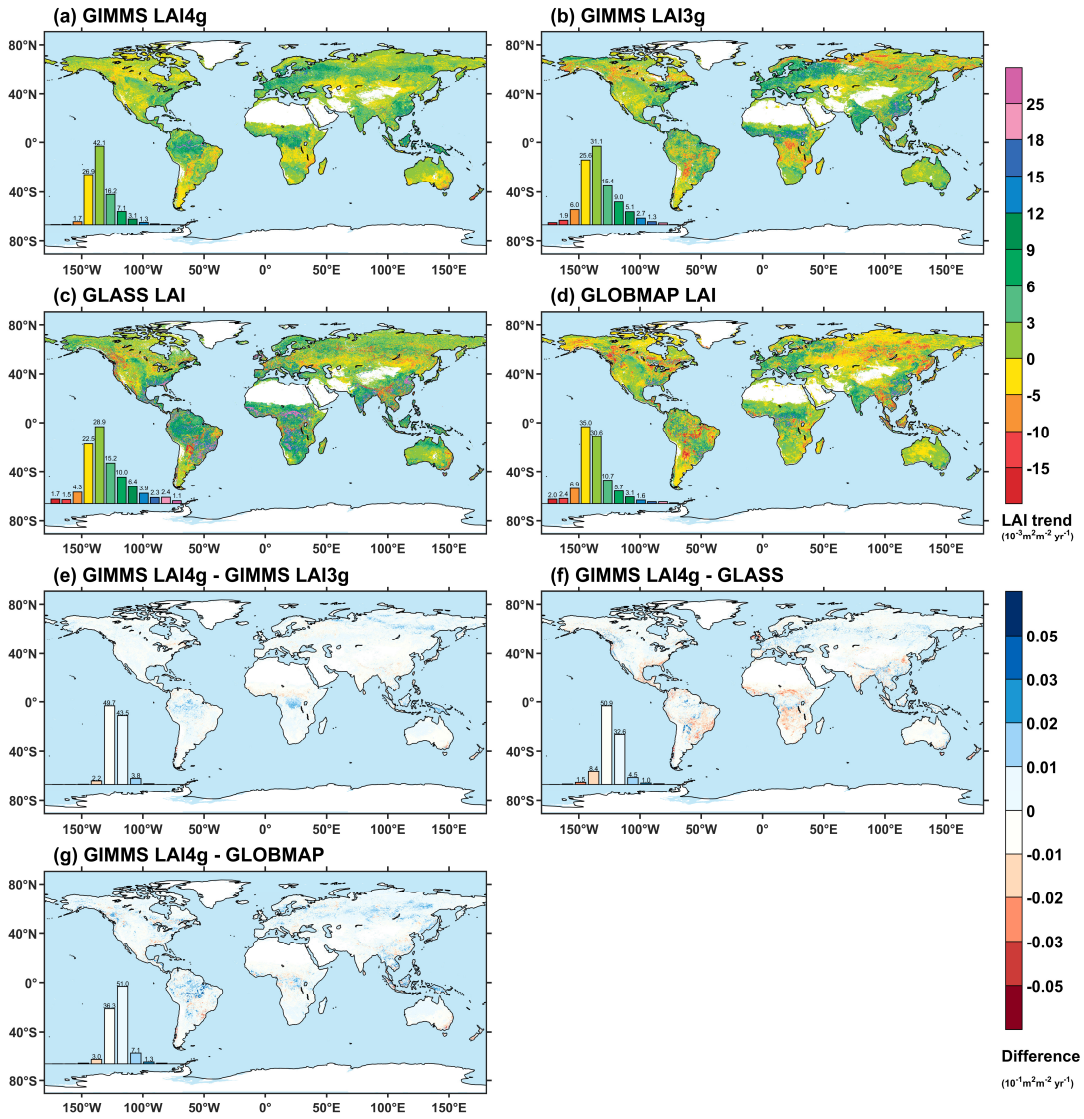

Figure 12. Global maps of LAI trends and their differences between the global LAI products during 1982−2015. The LAI products include GIMMS LAI4g after consolidation (a), GIMMS LAI3g (b), GLASS LAI (c), and GLOBMAP LAI (d). The trend was calculated as the slope of a linearly fitted LAI time series. (e) to (g) show the slope differences between the GIMMS LAI4g and the other three LAI products.

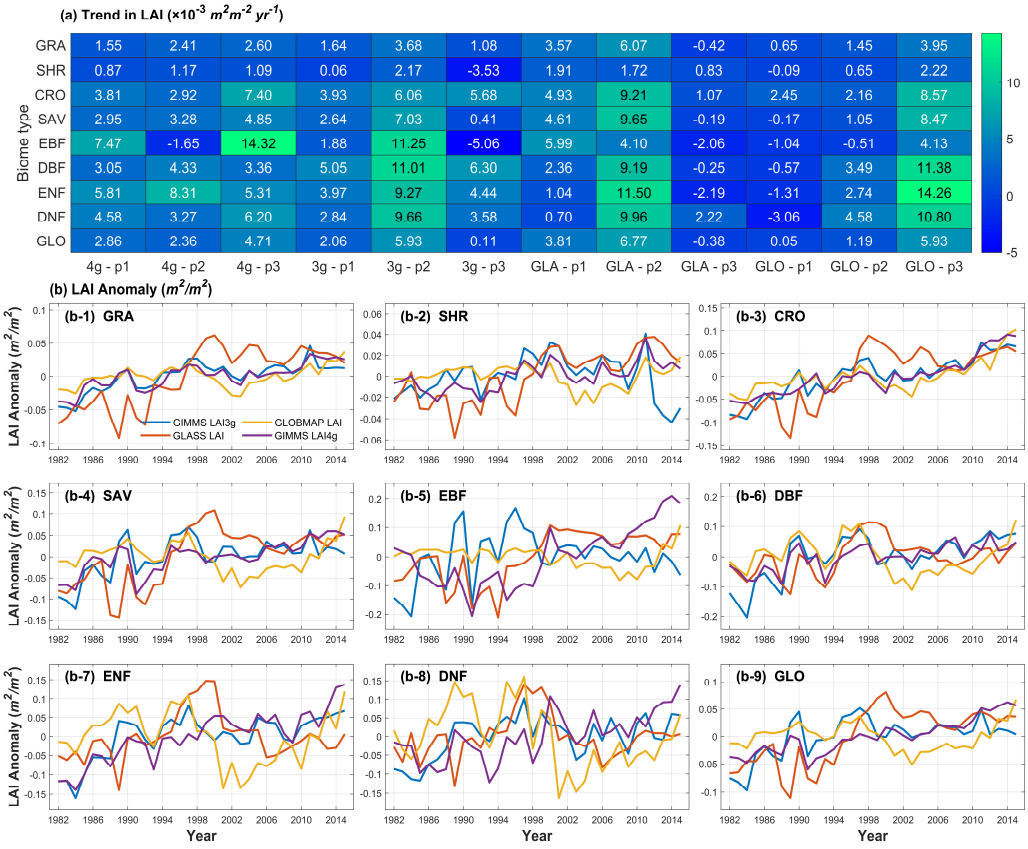

Figure 13. Variations of annual LAI anomaly of different vegetation biomes in the global LAI products during 1982−2015. The LAI products include GIMMS LAI4g, GIMMS LAI3g, GLASS LAI, and GLOBMAP LAI. (a) shows the slope values of the annual LAI during 1982−2020 (p1), 1982−2000 (p2), and 2001−2020 (p3). In the x-axis, 4g, 3g, GLA, and GLO stands for GIMMS LAI4g, GIMMS LAI3g, GLASS LAI, and GLOBMAP LAI, respectively. (b) shows the annual LAI time series.

Table 1 Error metric values for different combinations of explanatory variables (S1 to S5) in BPNN of each vegetation biome. Values in this table correspond to Figure 3. The combinations of explanatory variables are (S1) NDVI alone; (S2) NDVI and spatial information (longitude and latitude); (S3) NDVI, spatial information, and temporal information (month); (S4) NDVI, spatial information, temporal information, and NOAA satellite number; and (S5) NDVI, spatial information, temporal information, NOAA satellite number and years since its launch. GLO represents the global vegetation biome.

Metrics	combinations	Biome type								
		GRA	SHR	CRO	SAV	EBF	DBF	ENF	DNF	GLO
R^2	S1	0.76	0.86	0.68	0.66	0.09	0.64	0.49	0.63	0.91
	S2	0.79	0.88	0.77	0.73	0.36	0.74	0.56	0.65	0.92
	S3	0.83	0.91	0.83	0.81	0.52	0.87	0.65	0.78	0.95
	S4	0.83	0.91	0.84	0.81	0.53	0.87	0.68	0.79	0.95
	S5	0.83	0.91	0.84	0.82	0.53	0.87	0.68	0.80	0.95
RMSE (m^2/m^2)	S1	0.17	0.10	0.21	0.48	0.50	1.10	0.84	0.89	0.64
	S2	0.16	0.09	0.17	0.42	0.42	0.93	0.78	0.87	0.57
	S3	0.14	0.08	0.15	0.35	0.36	0.66	0.69	0.69	0.46
	S4	0.14	0.08	0.15	0.35	0.36	0.65	0.67	0.67	0.45
	S5	0.14	0.08	0.14	0.35	0.36	0.65	0.66	0.66	0.45
MAE (m^2/m^2)	S1	0.11	0.05	0.13	0.33	0.30	0.83	0.66	0.70	0.39
	S2	0.10	0.05	0.10	0.29	0.26	0.65	0.60	0.68	0.34
	S3	0.09	0.05	0.09	0.24	0.21	0.45	0.53	0.53	0.27
	S4	0.09	0.05	0.09	0.24	0.20	0.44	0.51	0.51	0.27
	S5	0.09	0.05	0.09	0.24	0.20	0.45	0.50	0.51	0.27
MAPE (%)	S1	24.36	16.75	28.06	23.09	5.06	24.60	23.16	24.33	17.61
	S2	22.18	15.95	22.59	19.82	4.33	19.29	21.16	23.40	15.40
	S3	19.85	14.55	19.17	16.50	3.51	13.15	18.64	18.26	12.27
	S4	19.88	14.36	19.11	16.45	3.44	13.09	17.94	17.73	12.02
	S5	19.88	14.45	19.03	16.46	3.43	13.16	17.79	17.56	11.98